Advanced Materials Research *Online: 2014-08-11*
ISSN: 1662-8985, Vol. 996, pp 33-38
doi:10.4028/www.scientific.net/AMR.996.33

X-ray diffraction profile analysis of high-heat-load materials

Mutsumi Sano[1a], Sunao Takahashi[1b], Atsuo Watanabe[1c], Ayumi Shiro[2d] and Takahisa Shobu[2e]

[1]JASRI SPring-8, 1-1-1 Kouto Sayo-cho, Sayo-gun, Hyogo 679-5198, Japan

[2]JAEA Quantum Beam Science Directorate, 1-1-1 Kouto Sayo-cho, Sayo-gun, Hyogo 679-5148, Japan

[a]musano@spring8.or.jp, [b]takahasi@spring8.or.jp, [c]watanaba@spring8.or.jp, [d]shiro.ayumi@jaea.go.jp, [e]shobu@spring8.or.jp

Keywords: profile analysis, X-ray diffraction, dislocation density, macro strain, synchrotron radiation

Abstract. An X-ray diffraction profile analysis was performed for GLIDCOP, dispersion-strengthened copper with ultra-fine particles of aluminum oxide. The Warrren-Averbach method was applied to a diffraction profile measured using synchrotron radiation. The dislocation density was evaluated from the analysis. The dislocation densities of GLODCOP with macro strains increased with increasing the strains.

Introduction

GLIDCOP, dispersion-strengthened copper with ultra-fine particles of aluminum oxide, is used as a material for high-heat-load components in SPring-8. In SPring-8 front ends this material has been applied to masks, absorbers [1], and XY slit assemblies [2]. All these components are typically subjected to a maximum power density of approximately 1 kW mm^{-2} at normal incidence for a standard in-vacuum undulator beamline. We have been investigating the fatigue property of GLIDCOP under cyclic high-heat-load conditions because the advancement of insertion devices has resulted in a progressive increase in the heat load [3]. As part of the investigation, strain measurements of the GLIDCOP samples were performed using synchrotron radiation [4,5]. We confirmed that the residual strains were almost in accordance with the FEM analyses in a previous study [4]. On the other hand, the plastic strain, which is the main cause of low cycle fatigue fracture phenomena, was evaluated by comparing the FWHM of the diffraction profile of samples with unknown plastic strain with that of samples with known plastic strain.

Recently, analysis of the X-ray diffraction profile has been one of the most powerful methods for investigating dislocation structure in plastically deformed materials [6]. In this study, a conventional Warren–Averbach method and a theory developed by Wilkens were employed to estimate the dislocation density [7,8]. The experiments were performed using synchrotron radiation X-rays. In particular, the internal dislocation density of a material can be nondestructively evaluated by using the synchrotron radiation. In this study we examined the dislocation density of GLIDCOP with the macro strain, i.e., compressive plastic strain.

Experiment

Two types of samples, TP1 and TP2, were used. Both test pieces were identical to those used in our previous studies [4,5]. Fig. 1 shows a schematic drawing of TP1, which comprises an absorbing body made of AL-15 grade GLIDCOP, as well as a fitting cover and a cooling holder made of stainless steel. An important feature of this assembly is its tapered configuration, which is adopted for localizing and concentrating the strain in the central area, thereby causing a low cycle fatigue fracture. Before performing experiments with synchrotron radiation, cyclic heat loads were applied to the central area of TP1 using an electron beam. Two samples with the TP1 configuration were prepared and subjected to different numbers of cycles: 50 and 100. The TP1 samples absorbed 550 W of power in each cycle; one cycle period comprised 7 min of thermal loading and 5 min of thermal unloading. On the other hand, the TP2 samples had known compressive plastic strains. The initial configuration

of the TP2 samples was a cylinder with a diameter of 15 mm and a height of 15 mm. These TP2 samples were manufactured with compressive plastic strains in the range 0–3.5 %. The central volumes of the TP2 samples, with thicknesses of 2 mm, were cut by electrical discharge machining after the compression stage. The average maximum temperatures of the TP1 samples were about 300 ºC during the heat cycles, while the compression stages of the TP2 samples were carried out at room temperature.

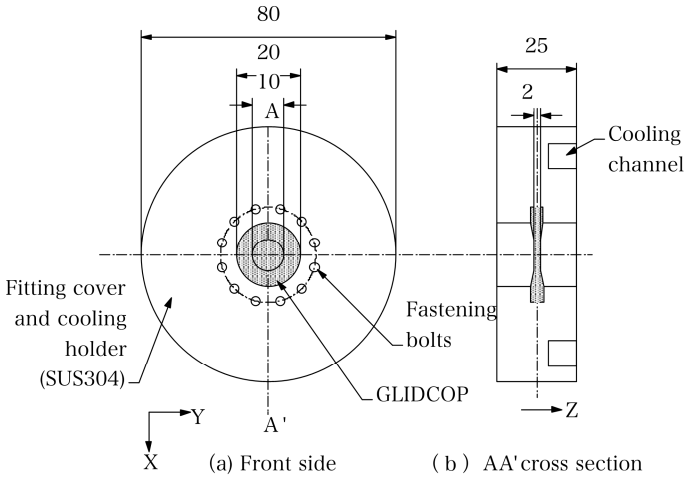

Figure 1: Schematic drawing of TP1.

The strain measurements were performed using a transmission-type strain scanning method in the beamline of BL02B1 at SPring-8. Fig. 2 and Table 1 show the configuration of the optics and X-ray specifications, respectively, used for the strain measurements. The measurements were conducted using Cu(200) and Cu(400) reflections and were performed at the center in every direction. Fig. 3 shows examples of the diffraction profiles for Cu(200) and Cu(400) reflections in the case of 1% plastic deformation of the TP2 sample.

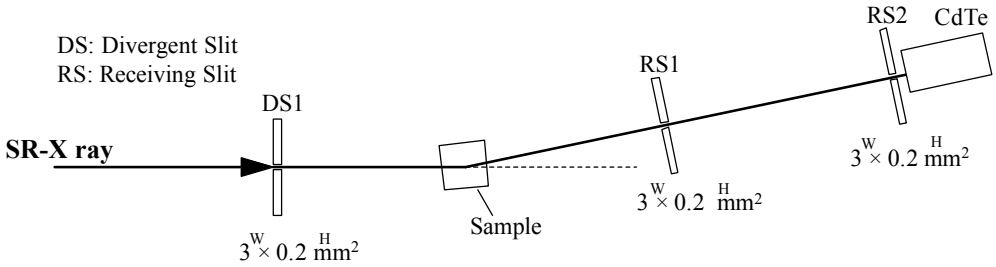

Figure 2: Optics used for strain measurements.

Table 1 X-ray specifications for strain measurements.

Beamline	SPring-8/BL02B1
Measurement method	Transmission-type strain scanning method
Energy	72.03 keV
Monochromatic crystal	Si(311)
Diffraction	Cu(200), Cu(400)
Diffraction angle, 2θ	5.45 deg (200), 10.92 deg (400)
Size of divergent slit 1 (Width × Height)	3 × 0.2 mm^2
Size of receiving slit 1 (Width × Height)	3 × 0.2 mm^2
Size of receiving slit 2 (Width × Height)	3 × 0.2 mm^2

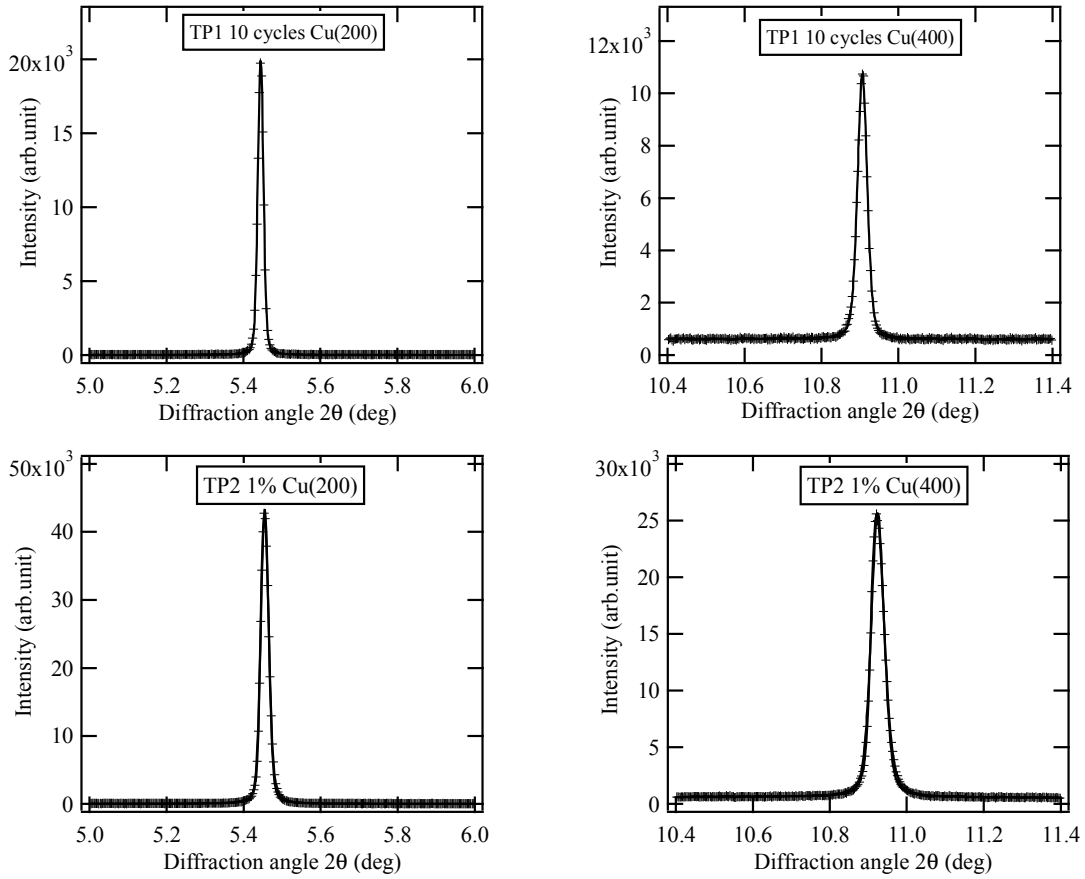

Figure 3: Cu(200) and Cu(400) diffraction profiles of the TP1 sample after 10 cycles and the TP2 sample with a compressive plastic strain of 1%. The marks represent experimental data; the solid line was obtained from a fitting of a pseudo-Voigt function with a linear background.

Diffraction Profile Analysis

The X-ray diffraction profiles were evaluated to obtain the dislocation density using the Warren–Averbach method [7]. The Fourier coefficient of each of the diffraction profiles can be expressed as the product of the size and the distortion coefficients, $\boldsymbol{A^s}$and $\boldsymbol{A^D}$, as follows:

$$A(L) = A^s \cdot A^D \tag{1}$$

Here, L is the Fourier length, defined as $L = na_3$, where n is an integer and a_3 is the unit of the Fourier length in the direction of the diffraction vector, as follows:

$$a_3 = \lambda/[2(\sin\theta_2 - \sin\theta_1)] \tag{2}$$

Here, the diffraction profile is measured from θ_1 to θ_2, and λ is the wavelength of the X-rays. The Fourier coefficients can be written as:

$$A(L) = A^s(L)(1 - 2\pi^2 L^2 \langle\varepsilon(L)^2\rangle/d^2), \tag{3}$$

where $\langle\varepsilon(L)^2\rangle$ is the mean square strain and d is the spacing. The mean square strain $\langle\varepsilon(L)^2\rangle$ can be written using two types of Fourier coefficients that correspond to the same lattice plane, such as (200) and (400), as follows:

$$\langle\varepsilon(L)^2\rangle = \left(d_{hkl}^2 d_{h'k'l'}^2/2\pi^2L^2\right) \cdot \left(A_{hkl}(L) - A_{h'k'l'}(L)\right)/\left(d_{hkl}^2 A_{hkl}(L) - d_{h'k'l'}^2 A_{h'k'l'}(L)\right) \tag{4}$$

Here, d_{hkl} and $d_{h'k'l'}$ represent the spacing for the (hkl) and $(h'k'l')$ reflections, respectively, and $A_{hkl}(L)$ and $A_{h'k'l'}(L)$ denote the Fourier coefficients for the (hkl) and $(h'k'l')$ reflections, respectively. For small values of L, $\langle\varepsilon(L)^2\rangle$ can be expressed as:

$$\langle\varepsilon(L)^2\rangle \cong (\rho\bar{C}b^2/4\pi)\ln R_e - (\rho\bar{C}b^2/4\pi)\ln L, \quad (5)$$

where ρ is the dislocation density, R_e is the effective outer cut-off radius, b is the absolute value of the Burgers vector, and $\bar{C}$ is the average contrast factor of the dislocations [8]. In the cubic crystal system, the average contrast factor $\bar{C}$ can be written as:

$$\bar{C} = \bar{C}_{h00}(1 - qH^2), \quad (6)$$

where $\bar{C}_{h00}$ is the average contrast factor corresponding to the (h00) reflection, q is a constant, and $H^2 = (h^2k^2 + h^2l^2 + k^2l^2)/(h^2 + k^2 + l^2)$ [9].

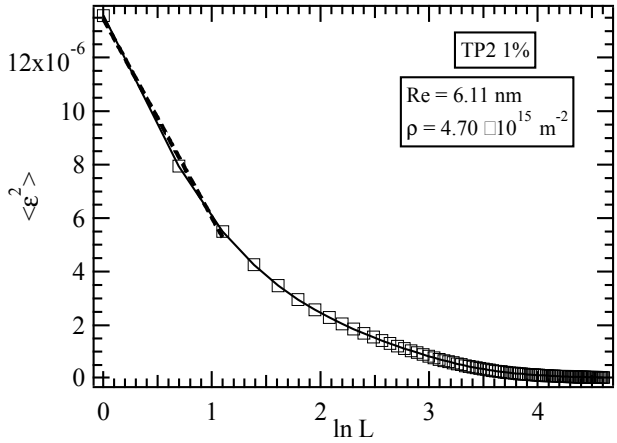

Figure 4: Relationship between $\langle\varepsilon(L)^2\rangle$ and ln L in TP2 samples with a compressive plastic strain of 1%. The dotted line was obtained from a fitting of Eq. 5.

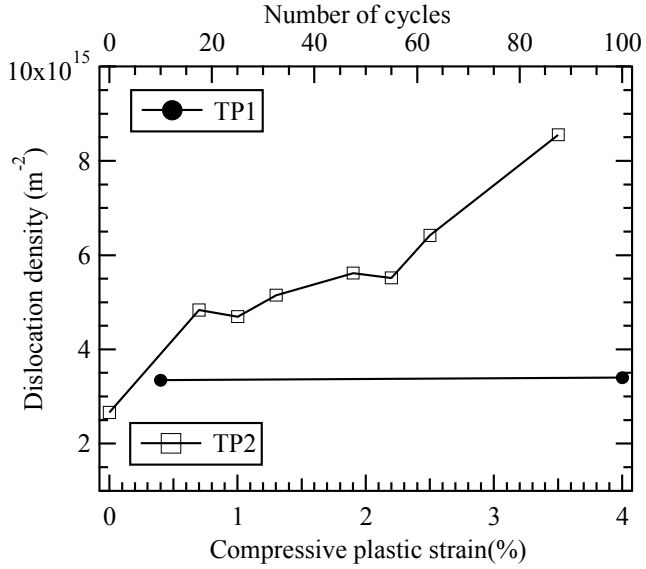

Figure 5: Dislocation densities of TP1 and TP2 samples. The bottom and top axes show the compressive plastic strains for the TP2 samples and the number of cycles of the TP1 samples, respectively.

A pseudo-Voigt function with a linear background was fitted to the profiles of the Cu(200) and Cu(400) reflections, as shown in Fig. 3. The cosine Fourier coefficients $A_{200}(L)$ and $A_{400}(L)$ and the spacings d_{200} and d_{400} were obtained from the fitting functions. In this study, we assumed that the instrumental line broadening was negligible, because the instrumental line broadening of the

beamline was expected to be less than 0.002º from the previous study [9]. The plot of $\langle \varepsilon(L)^2 \rangle$ obtained from Eq. 4 versus ln L is shown in Fig. 4. The straight line fitted to small values of L for Eq. 5 provided the dislocation density ρ and the effective outer cut-off radius R_e. The value of 0.304 was adopted as the average contrast factor $\bar{C}_{h00}$ of copper [10].

Fig. 5 shows the dislocation densities of the TP1 and TP2 samples. The bottom and top x-axes show the compressive plastic strains for the TP2 samples and the number of cycles for the TP1 samples, respectively. The dislocation densities of the TP2 samples ranged from 2.7×10^{15} to 8.6×10^{15} m^{-2}; this value increases with increasing compressive strain. In contrast, these values for the TP1 samples are almost constant at approximately 3.4×10^{15} m^{-2} for any number of heat cycles.

Discussion

FEM calculations for the TP1 samples indicated that the compressive strain was constant at approximately 1.8% for more than eight cycles [4,5]. We confirmed that the FEM calculations were appropriate by using the results of the fatigue-life experiments and the residual strain measurements [3,4]. We are planning to evaluate the compressive plastic strains of the TP1 samples by comparing the dislocation densities of the TP2 samples with those of the TP1 samples. However, after evaluating the plastic strain of the TP1 samples from the present results shown in Fig. 5, we found that these values are too small. Some reasons for this difference are as follows. The temperatures when applying the compressive plastic strains were very different between the TP1 and TP2 samples. This situation may cause the different dislocation densities between the two samples even if the compressive plastic strains have the same value. Moreover, the dislocation densities obtained from the present analysis were evaluated by the conventional Warren–Averbach method using only (200) and (400) reflections. We suppose that to improve the accuracy of the analysis, modified Williamson–Hall and modified Warren–Averbach method including the consideration of the instrumental line broadening must be applied to the analysis [6].

Summary

We estimated the dislocation densities of TP1 and TP2 samples using X-ray diffraction profiles by applying the Warren–Averbach method. The dislocation densities of the TP1 samples were almost constant, while those of TP2 samples increased with increasing the compressive plastic strain. Further investigations will be needed in order to estimate the absolute values of the dislocation densities.

Acknowledgement

The synchrotron radiation experiments were performed at the SPring-8 with the approval of the Japan Synchrotron Radiation Research Institute (JASRI) (Proposal No. 2013A1718).

References

[1] T. Mochizuki, Y. Sakurai, D. Shu, T.M. Kuzay, H. Kitamura, Design of compact absorbers for high-heat-load X-ray undulator beamlines at SPring-8, J. Synchrotron Rad. 5 (1998) 1199-1201.

[2] M. Oura, Y. Sakurai, H. Kitamura, Front-end XY-slits assembly for the SPring-8 undulator beamlines, J. Synchrotron Rad. 5 (1998) 606-608.

[3] S. Takahashi, M. Sano, T. Mochizuki, A. Watanabe, H. Kitamura, Fatigue life prediction for high-heat-load components made of GlidCop by elastic-plastic analysis, J. Synchrotron Rad. 15 (2008) 144-150.

[4] M. Sano, S. Takahashi, A. Watanabe, H. Kitamura, K. Kiriyama, T. Shobu, Internal residual strain of GlidCop for materials of the high-heat-load components, Materials Science Forum, 652 (2010) 222-226.

[5] M. Sano, S. Takahashi, A. Watanabe, H. Kitamura, S. Shiro, T. Shobu, Plastic strain of GlidCop for materials of high heat load components, Materials Science Forum, 772 (2014) 123-127.

[6] T. Ungar, A. Borbely, The effect of dislocation contrast on x-ray line broadening: A new approach to line profile analysis, Appl. Phys. Lett. 69 (1996) 3173-3175.

[7] B.E. Warren, X-ray studies of deformed metals, Prog. Met. Phys. 8 (1959) 147-202.

[8] M. Wilkens, Fundamental Aspects of Dislocation Theory, Nat. Bur. Stand. Spec. Publ., USA, No. 317, Vol. II, 1970, 1195-1221.

[9] Y. Noda, Current Status of Crystal Structure Analysis BL02B1 Experimental Station, SPring-8 INFORMATION, Volume 02, No.5 (1997) 17-23.

[10] T. Ungar, I. Dragomir, A. Revesz, A. Borbely, The contrast factors of dislocations in cubic crystals: the dislocation model of strain anisotropy in practice, J. Appl. Cryst. 32 (1999) 992-1002.